

Genome comparison of *Candida orthopsilosis* clinical strains reveals the existence of hybrids between two distinct subspecies

Leszek P. Pryszcz^{1,2}, Tibor Németh³, Attila Gacser^{3*}, and Toni Gabaldón^{1,2,4*}

1) Bioinformatics and Genomics Programme. Centre for Genomic Regulation (CRG). Dr. Aiguader, 88. 08003 Barcelona, Spain

2) Universitat Pompeu Fabra (UPF). 08003 Barcelona, Spain.

3) University of Szeged, Department of Microbiology, Közép fasor 52, H-6726 Szeged, Hungary

4) Institució Catalana de Recerca i Estudis Avançats (ICREA), Pg. Lluís Companys 23, 08010 Barcelona, Spain.

* both authors share senior authorship: gacsera@gmail.com, tgabaldon@crg.es,

Running title

Candida orthopsilosis clinical hybrids

© The Author(s) 2014. Published by Oxford University Press on behalf of the Society for Molecular Biology and Evolution.

This is an Open Access article distributed under the terms of the Creative Commons Attribution License (<http://creativecommons.org/licenses/by/3.0/>), which permits unrestricted reuse, distribution, and reproduction in any medium, provided the original work is properly cited.

Abstract

The *Candida parapsilosis* species complex comprises a group of emerging human pathogens of varying virulence. This complex was recently subdivided into three different species: *C. parapsilosis* sensu stricto, *C. metapsilosis*, and *C. orthopsilosis*. Within the latter, at least two clearly distinct subspecies seem to be present among clinical isolates (Type 1 and Type 2). To gain insight into the genomic differences between these subspecies we undertook the sequencing of a clinical isolate classified as Type 1 and compared it to the available sequence of a Type 2 clinical strain. Unexpectedly, the analysis of the newly sequenced strain revealed a highly heterozygous genome, which we show to be the consequence of a hybridization event between both identified subspecies. This implicitly suggests that *C. orthopsilosis* is able to mate, a so-far unanswered question. The resulting hybrid shows a chimeric genome which maintains a similar gene dosage from both parental lineages and displays ongoing loss of heterozygosity. Several of the differences found between the gene content in both strains relate to virulent-related families, with the hybrid strain presenting a higher copy numbers of genes coding for efflux pumps or secreted lipases. Remarkably, two clinical strains isolated from distant geographical locations (Texas and Singapore) are descendants of the same hybrid line, raising the intriguing possibility of a relationship between the hybridization event and the global spread of a virulent clone.

Introduction

Although *C. albicans* remains the main cause of invasive candidiasis cases, clinical data indicate that the members of the *C. parapsilosis* complex are significant pathogens with increasing prevalence (van Asbeck et al. 2009). This species complex was recently recognized to contain three closely related species, formerly distinguished as *C. parapsilosis* group I, group II and

group III, which became known as *C. parapsilosis sensu stricto*, *C. orthopsilosis* and *C. metapsilosis*, respectively (Tavanti et al. 2005). Although the three species are closely related, they differ markedly in their clinical prevalence, virulence and antifungal susceptibility. However, all three species are able to cause serious conditions with various clinical manifestations, including fungaemia (Lockhart et al. 2008). Several epidemiological studies indicate that the majority of *C. parapsilosis* complex infections is caused by *C. parapsilosis sensu stricto* isolates, and *C. orthopsilosis* is responsible for about 1-10 % of cases depending on the geographic region (Lockhart et al. 2008). However, *C. orthopsilosis* is more frequently identified than *C. metapsilosis* (Riccombeni et al. 2012; Bonfietti et al. 2012), although both species have been associated with several outbreaks of infection in addition to sporadic cases (Lockhart et al. 2008; Taj-Aldeen et al. 2013; Ge et al. 2012). While the commensal status of *C. parapsilosis sensu stricto* in humans is well known, that of the other two species from the *C. parapsilosis* complex has not been confirmed yet, although a metagenomic study indicated the presence of *C. metapsilosis* in the oral cavity of healthy human subjects (Ghannoum et al. 2010).

Despite their clinical importance, there are relatively few studies investigating the virulence of the *C. parapsilosis sensu lato* species, specially for *C. orthopsilosis* and *C. metapsilosis*. To date, only few studies have been conducted to compare the virulence of *C. parapsilosis sensu stricto*, *C. orthopsilosis* and *C. metapsilosis* isolates. Most studies generally indicate that, for the conditions tested, *C. orthopsilosis* displays virulence and adhesion properties similar to *C. parapsilosis*, whereas *C. metapsilosis* is the least virulent species (Bertini et al. 2013; Gácsér, Schäfer, et al. 2007; Orsi et al. 2010; Butler et al. 2009). The most extensive study to date examining the virulence of the three species using *in vitro* and *in vivo* infection systems

determined that *C. orthopsilosis* and *C. metapsilosis* isolates were less resistant to killing by human macrophages compared to *C. parapsilosis sensu stricto* strains (Németh et al. 2013). In addition, this study analyzed the producing capacity, in several strains of each species, of extracellular protease and lipase (both known as important virulence factors during *Candida* infections (Gácsér, Trofa, et al. 2007; Monod & Borg-von 2002). Their results showed that, while the majority of *C. parapsilosis sensu stricto* strains were positive for both lipase and protease production, only a small number of *C. orthopsilosis* and none of the *C. metapsilosis* isolates were able to produce lipases.

Considering that virulence properties can vary significantly among strains of the same species, it is important to study the detailed genetic background of pathogenic isolates. This aspect seems to be of particular importance for *C. orthopsilosis*, where initial analyses of ITS region and MAT-cassette genes have shown that this species is formed by at least two clearly distinguishable subspecies: called Type 1 and Type 2 (Sai et al. 2011). The genome sequence of *C. parapsilosis sensu stricto* has been available since 2009 (Butler et al. 2009), facilitating numerous studies on the biology and virulence of this species. Recently, the first genome-wide comparison of several *C. parapsilosis* strains was published, shedding light onto the population structure of this species (Pryszcz et al. 2013). The genome of a Type 2 *C. orthopsilosis* was sequenced only in 2012 (Riccombeni et al. 2012), which served to compare it extensively with that of *C. parapsilosis*. The main differences found included an expansion of the Hyr/Iff family of cell wall genes and the JEN family of monocarboxylic transporters in *C. parapsilosis* relative to *C. orthopsilosis*. However, the lack of sequences from additional strains, in particular from the other identified subspecies, has prevented gaining insight into the genomic variability within this species. To fill

in this important gap, we undertook the sequencing of a *C. orthopsilosis* clinical isolate assigned to Type 1, a different subspecies than that of the reference strain, and compared both sequences. Our results indicate that the newly sequenced isolate is likely to represent a hybrid between the two *C. orthopsilosis* subspecies. In addition, we find no increase in ploidy and evidence of meiotic recombination between the different haplotypes, strongly suggesting the existence of mating among different *C. orthopsilosis* lineages. Strikingly, this hybrid lineage is represented by at least two clinical isolates from distant continents, suggesting a global spread. In addition we found several differences in virulence related gene families between the two strains, pointing to a larger copy number of efflux pumps and secreted lipases in the hybrid. These findings raise the question of the possible role that the formation of hybrids may have in the success and spread of virulent strains. Future analyses are need to clarify the population structure of this poorly sampled species.

Material and Methods

DNA extraction

C. orthopsilosis cultures were grown overnight in an orbital shaker (200 rpm, 30 °C) in 2 ml YPD medium (0,5% yeast extract, 1% peptone, 1% glucose) supplemented with 1% penicillin-streptomycin solution (Sigma). Then, cells were centrifuged (3000 rpm, 5 minutes) and were washed twice with 1x sterile PBS. The pellett was resuspended in 500 µl lysis buffer (1 w/V% SDS, 50mM EDTA, 100 mM TRIS pH=8), 500 µl glass bead was added to the cells and were disrupted by using a vortex for 3 minutes. 275 µl 7M ammonium-acetate was added (65 °C, 5 min) and the samples were cooled on ice for 5 minutes. Then 500 µl of chloroform-

isoamylalcohol (24:1) was added to the mixture, which was then centrifuged for 10 minutes at 13000 rpm. The upper phase was transferred to a new microcentrifuge tube, and the previous step was repeated. 500 μ l isopropanol was mixed with the upper phase in a new microcentrifuge tube, and the mixture was held in a refrigerator at -20 °C for 5 minutes. The solution was centrifuged at 13000 rpm for 10 minutes. The supernatant was discarded, and the pellet was washed twice with 500 μ l 70 % ethanol. After the second washing step the pellet was dried, and was resuspended in 100 μ l bi-distilled water containing RN-ase (Sigma).

Sporulation assay

Ascospore formation was investigated under the microscope using various sporulation media (Sporulation medium: 0.5% Na-acetate, 0.5% KCl, 0.1% yeast extract, 0.05% glucose, 2% agar; Spider medium: 1% mannitol, 1% nutrient broth, 0.2% K₂HPO₄, 1.5% agar, at different pH (pH 4, pH 5, pH 7, pH 8, pH 9) adjusted with Me Ilvaine buffer solutions; Minimal medium supplemented with different C-source: 1% YNB (yeast nitrogen base), 2% galactose or 2% maltose or 2% L-sorbose or 2% D-sorbitol or 2% glycerol + 2% agar). The plates were incubated at 25°C, 30°C, 37°C, or at 37°C with 5% CO₂ and 100% humidity. The ascospore formation was followed by microscopic observation after 5, 10, 14, 21 and 35 days after inoculation.

Genome sequencing

The genome for this strain was obtained at the Ultra-sequencing core facility of the CRG, using Illumina GAIIx sequencing machine. DNA was fragmented by nebulization or in Covaris to a size ~300 bp. After shearing, the ends of DNA fragments were blunted with T4 DNA polymerase and Klenow fragment (New England Biolabs). Then, DNA was purified with a QIAquick PCR purification kit (Qiagen). Thereafter, 3'-adenylation was performed by

incubation with dATP and 3'-5'-exo- Klenow fragment (New England Biolabs). DNA was purified using MinElute spin columns (Qiagen) and double-stranded Illumina paired-end adapters were ligated to the DNA using rapid T4 DNA ligase (New England Biolabs). After another purification step, adapter-ligated fragments were enriched, and adapters were extended by selective amplification in an 18-cycle PCR reaction using Phusion DNA polymerase (Finnzymes). Libraries were quantified and loaded into Illumina flow-cells at concentrations of 7-20 pM. Cluster generation was performed in an Illumina cluster station. Sequence runs of 2×76 cycles were performed on the sequencing instrument. Base calling was performed using Illumina pipeline software. In multiplexed libraries, we used 4 bp internal indices (5' indexed sequences). De-convolution was performed using the CASAVA software (Illumina).

Genome assembly

Reads were pre-processed before assembly to trim at the first undetermined base or at the first base having PHRED quality below 10. The pairs with one (or both) reads shorter than 31 bases after trimming were excluded from the assembly process. SOAPdenovo2 (Luo et al. 2012) was used to assemble paired-ends reads into supercontigs, using K-mer ranging from 31 to 63. As the initial assembly was very fragmented (6,827 contigs) and larger (15.6 Mb) than of the reference strain (12.6 Mb), we assumed the presence of heterozygous regions in our strain (Table 1). Heterozygous regions (3 Mb, 4,668 contigs) were successfully removed by Haplomerger version 20120810 (Huang et al. 2012). Subsequently, remaining supercontig were further scaffolded by SSPACE2 (Boetzer et al. 2011) and gaps were filled using GapCloser from SOAPdenovo package. Finally, supercontigs were scaffolded on *C. orthopsilosis* 90-125 chromosomes using Oslay version 1.0 (Richter et al. 2007).

Genome annotation

Genes were predicted using Augustus version 2.5.5 (Stanke et al. 2006) using *C. parapsilosis* CDC317 gene models for training. Predicted gene models were curated using RNA-Seq reads (accession PRJEB5019) by means of exon-intron boundaries and exon skipping. Subsequently, we grouped predicted genes into orthogroups and transferred functional annotation from one-to-one orthologs in model species ie. *Candida albicans* or *Saccharomyces cerevisiae*, based on predictions from the MetaPhOrs approach (Pryszcz et al. 2011). Finally, genes were further annotated using InterProScan 5RC4 (Quevillon et al. 2005).

Detection of SNPs, loss of heterozygosis, and divergence estimates

MCO456 reads were aligned onto *C. orthopsilosis* 90-125 chromosomes using Bowtie2 with “very sensitive local alignment” mode (Langmead & Salzberg 2012). SNPs and INDELs were called using GATK version 2.1-13 (McKenna et al. 2010). We filtered out clusters of 5 variants within 20 bases and low quality variants, as described in GATK documentation (QD < 2.0 || MQ < 40 || FS > 60.0 || HaplotypeScore > 13.0 || MQRankSum < -12.5 || ReadPosRankSum < -8.0). Subsequently, we divided variants into two groups: homo- and heterozygous. Firstly, we marked parts of MCO456 genome having lower or higher (allowing 25% deviation) coverage than expected as unknown (10%). Then, we defined heterozygous regions as regions having two or more heterozygous sites in given strain closer than 100 bases. The remaining regions of the genome were considered homozygous, thus the results of loss of heterozygosity (LOH). By analysing alignments of assembled contig sequences, we initially obtained 99.69% identity between AY2 and MCO456. However, this value may be inflated due to errors in base calls in

the assembly. We thus used an alternative strategy consisting in aligning MCO456 reads onto AY2 contigs using BWA MEM version 0.7.5a (Li & Durbin 2010) to call SNPs as previously described. This rendered a higher identity between MCO456 and AY2: 99.9733% (3,369 homozygous SNPs). This should still be considered a minimal estimate because the lack of raw reads for AY2 prevents us from doing a similar correction of that assembly. Assuming similar base call error rate in the two strains, the identity between AY2 and MCO456 should be considered 99.997%. Finally, the distributions of frequencies of read counts at biallelic SNPs were analyzed to estimate ploidy of each chromosome. For this, SNP calls were further filtered ignoring: i) bases with quality lower than 20, ii) bases in reads with mapping quality lower than 15, and iii) positions with less than 20 reads mapped.

Detection of structural variants

Structural variants were detected using a methodology described and experimentally validated elsewhere (Pryszcz et al. 2013). In brief variants were first detected using the Delly package (Rausch et al. 2012) and then carefully curated as explained below. In addition, we performed independent analyses based on depth of coverage to detect duplications and deletions not identified by Delly. For every *C. orthopsilosis* gene, we computed number of reads per kilobase of coding sequence per million of aligned reads (RPKM). For any given sequencing experiment, RPKM is expected to be constant unless it is affected by duplication or deletion. We defined a gene being duplicated in a given strain if \log_2 of observed versus expected RPKM for that gene was greater than 0.75. Similarly, we called putative deletions if \log_2 ratio was smaller than -0.75. Obtained ratios allow not only the detection of duplication/deletions, but also inform about the number of copies that are gained or lost. Finally, we used split-reads as additional line of

evidence. We split in two the reads that were aligned over less than 90% of their length and subsequently re-aligned these. Alignments created in this way were often flanking putative structural variants. All detected variants were manually curated by visual inspection of the aligned reads. In addition, we generated genome graphs for all chromosomes illustrating copy number variation, and homozygous and heterozygous mutations densities (Supplementary file 3). Surprisingly, over half of the identified duplications were shared by *C. orthopsilosis* 90-125 and MCO456. These duplications were not correctly resolved in the reference assembly (90-125) due to the low level of divergence between the two paralogous regions and resulted in assembly gaps (Supplementary figure S1). Inferred assembly gaps are consistently smaller than the nearby duplicated regions, suggesting this was the result of a tandem duplication and pointing to a possible strategy to close these gaps in the reference assembly.

Phylogenetic analyses

Concatenated alignment of heterozygous contigs from *C. orthopsilosis* MCO456 and their orthologous regions from *C. orthopsilosis* AY2 and *C. orthopsilosis* 90-125 were generated using Mugsy v1r2.3 (Angiuoli & Salzberg 2011). The resulted alignment consisted of 1,432,069 columns. In order to root the tree, we performed an additional analysis with the subset of regions that could be aligned to corresponding orthologous regions in *C. parapsilosis* CDC317. This alignment resulted in 632,907 columns. Maximum Likelihood phylogenetic trees were reconstructed using RAxML 7.2.8 using GTRCAT model (Stamatakis et al. 2005).

Results and Discussion

Genome sequencing and annotation of the MCO456 strain

Previous work, based on ITS and MAT loci divergence, has established that most *C. orthopsilosis* strains belong to two clearly distinct subspecies, referred to as Type 1 and Type 2 (Sai et al. 2011). The recently sequenced *C. orthopsilosis* reference strain (90-125; from California, USA) belongs to Type 2 (Riccombeni et al. 2012). Here, we sequenced *C. orthopsilosis* strain MCO456 (ATCC96141) originally isolated from a blood sample in San Antonio (Texas, USA). This strain can be classified as the alternative Type 1 subspecies based on phylogenetic analyses of the ITS region and *MTL* α idiomorphs (Supplementary figures S2 and S3). The resulting assembly comprises 116 scaffolds and a 544x coverage (Table 1, accession PRJEB4430). Automated annotation resulted in 5,756 predicted genes, grouped into 5,279 orthologous groups (including orthologs, and in-paralogs), which is roughly similar to the reference strain (Table 1). 4,691 orthologous groups are common to *C. parapsilosis* and the two *C. orthopsilosis* strains. Of these, 4,258 are present precisely in one copy in each of these genomes (one-to-one orthologs). The main gene content differences between *C. orthopsilosis* and *C. parapsilosis* have been previously described for the reference strains (Riccombeni et al. 2012). Most such observations are confirmed for the newly sequenced strain. In some cases the new sequence helps to expand this observations. For instance, the cell-wall assembly protein family Hyr/Iff has been expanded in *C. parapsilosis* relative to *C. orthopsilosis*, although the exact number of copies in the latter could not be determined due to the presence of gaps in the relevant assembly region (Riccombeni et al. 2012). We confirm such finding for the strain sequenced here, in which the absence of assembly gaps in the Hyr/Iff positions allows us to determine the number of copies to four, as compared to 17 in *C. parapsilosis*. Most of the

differences in gene content correspond to differences in copy number within gene families, and others that can be attributable to differences in annotation or coverage between the two assemblies (Supplementary table S1). We focused on differences between the two strains that are supported by reciprocal mapping of raw reads and are therefore independent of differences in the assembly and/or the annotation procedures. Importantly, several of these well supported differences correspond to virulence-related gene families (see below).

Structural and gene content variations between 90-125 and MCO456 strains

Using a re-mapping strategy, we identified structural variants in both sequenced *C. orthopsilosis* strains (see Materials and Methods). Altogether, we identified 29 duplications (Supplementary table S2) and 103 deletions (Supplementary table S3). Over half of the identified duplications (17) were shared by *C. orthopsilosis* 90-125 and MCO456 and correspond to collapsed regions in the published assembly of 90-125. By using pair-end mapping information we could infer that at least 17 out of the 29 detected duplications were intra-chromosomal and that the additional copy is likely to be placed several kb up- or downstream, coinciding with nearby gaps in the reference assembly (Materials and Methods, and Supplementary figure S1). The largest duplication (DUP2, a segmental duplication of 238 kb) was found in *C. orthopsilosis* 90-125 and represents a collapsed region in the reference assembly (Supplementary figure S4). This duplication is located at chromosome HE681719 and affects 74 genes (Supplementary table S4). Besides the rRNA cluster (DUP29), the gene expansion involving the highest number of paralogous copies (5-6x, DUP28) was found in *C. orthopsilosis* MCO456 and affected the gene CORT_0H02780, which encodes a putative outer-membrane Na/K efflux pump. The resulting ~12 copies of the gene - as compared to just two copies in 90-125 - are distributed over five

chromosomes and are all identical at the nucleotide level, pointing to a recent expansion. A large fraction of the identified deletions (85 out of 103) are homozygous, 43 affect coding genes and five result in putative gene fusions. Similar to what has been reported for *C. parapsilosis* (Pryszcz *et al.* 2013), a significant number of deletions [40] were surrounded by DNA direct repeats, suggesting Single Strand Annealing (SSA) as the prevalent mechanism of DNA double strand break (DDSB) repair in *C. orthopsilosis* (Ivanov *et al.* 1996). The largest deletion (DEL51) is 7,300 bp long and is surrounded by 824 bases long direct repeats. The two genes flanking this deletion (CORT_0C02740 and CORT_0C02745) are both co-orthologous to *C. albicans* Iff5, a GPI-anchored, adhesin-like protein. Interestingly, Iff5 has been expanded in *C. orthopsilosis* 90-125 and *C. parapsilosis*, but *C. orthopsilosis* MCO456 encodes only one copy due to this deletion.

446 gene families differ in the number of members between any of *C. orthopsilosis* strains or *C. parapsilosis* (Supplementary table S1). Of these, 239 contain more members in MCO456 than in 90-125, whereas only 56 contain more members in 90-125 than in MCO456. Notably, Iff5 seems to be the only virulence related gene family that is present in a higher number of copies in 90-125 strain, as compared to MCO456. For several other virulence-related gene families the newly sequenced strain presented lineage-specific expansions. For instance, MCO456 shows a significantly larger number of efflux pumps from the Major Facilitator Superfamily (MFS) with 142 MFS-coding genes distributed across 83 different MFS clades, as compared to 128 in 90-125 (Supplementary table S1). Thus MCO456 efflux-pump toolkit is closer to that of *C. parapsilosis* (147 members). Similarly *C. orthopsilosis* MCO456 have two additional Secreted Aspartic Proteases (SAPs), which have been associated with *C. albicans* and *C. parapsilosis* virulence,

through their involvement in the degradation of components of the innate immune system and survival in macrophages (Naglik et al. 2003; Horváth et al. 2012), with 25 SAP-coding genes, as compared to 23 in 90-125 and 26 in *C. parapsilosis* (Supplementary table S1). Finally, *C. orthopsilosis* MCO456 strain displays a specific duplication of a cluster of lipases resulting in four members, as compared to two in 90-125 and *C. parapsilosis* (Supplementary table S1, cluster#30). This finding is particularly interesting, since secreted fungal lipases are thought to have a role in many virulence associated processes, including nutrient acquisition by liberation of free fatty acids from lipid molecules, adhesion to host cells and generation of inflammatory mediators, and differences in the ability to secrete lipases among *C. orthopsilosis* strains have been noted (Gácsér, Stehr, et al. 2007). Although the actual relevance to virulence properties of these genomic differences remains to be established, it is nevertheless remarkable that several of the few differences found between the strains consistently hint towards an expanded virulence toolkit in MCO456. Notably, we have previously investigated the virulence of the MCO456 strain in vitro, along with other *C. orthopsilosis* isolates (Németh et al. 2013). It forms pseudohyphae and produces extracellular proteinases, but lacks extracellular lipase activity, similarly to other *C. orthopsilosis* strains. Furthermore, the phagocytosis of MCO456 strain by J774.2 mouse macrophages was comparable to the phagocytosis of *C. parapsilosis sensu stricto*. Similarly, some of the differences in gene content hint to families involved in drug resistance (see Supplementary table S1). This includes six more members in MCO456, than in 90-125, of the amino acid permease DIP5 involved in resistance to ergosterol analogs in *C. albicans* (Xu et al. 2007), six more members of the Pleiotropic drug resistance (PDR) subfamily of ABC transporters, and three more members of the major facilitator superfamily transporters and of homologs of SEC7, all of them families related to “response to drug” processes in *C. albicans*,

according to Candida Genome Database (Binkley et al. 2014). Finally, MCO456 carry five mutations in ERG3 (CORT_0E05900), a gene frequently found mutated in *C. albicans* strains resistant to azoles (Martel et al. 2010), including two affecting the promoter and one non-synonymous mutation (Y13C). Again, assessing whether these genomic differences effectively confer some increased resistance to anti-fungal drugs, needs to be established experimentally. Susceptibility to some drugs has only been studied in MCO456 in a comparative analysis with other *C. parapsilosis* complex species (Szenzenstein et al. 2013). In that study MIC₁₀₀ value in liquid medium (100% growth inhibition) of atorvastatin was 25 mg mL⁻¹ for *C. parapsilosis* and 50 mg mL⁻¹ for *C. orthopsilosis* (MCO456). *C. orthopsilosis* MCO456 was found to be the less susceptible to fluvastatin as compared to *C. parapsilosis* and *C. metapsilosis*, as 12.5 mg mL⁻¹ concentration caused only 50% growth inhibition. Direct comparison of the two sequenced-strains in terms of virulence and antifungal resistance properties is needed to establish whether the hybridization is associated to changes in these phenotypes.

***C. orthopsilosis* MCO456 is a hybrid between two distinct subspecies.**

The most striking observed difference between the two strains, however, was the high degree of heterozygosity found in MCO456 with a total of 2,182 kb heterozygous sites, representing 17% of the genome), as compared to the very low fraction of heterozygous sites in 90-125 (12.6 kb, 0.1%). The heterozygous sites in MCO456 are clustered in 4,872 regions that show an average inter-allelic divergence of 4.5%. Interestingly, the distribution of distances to 90-125 in MCO456

homozygous regions is bimodal (Figure 1A): 5,169kb (41%) of the genome is nearly identical to 90-125 genome (0-18 SNPs per 1kb, this is $\leq 1.8\%$ divergence) with an average divergence of 1.12% and 4,015kb (32%) is diverged above 1.8% (more than 18 SNPs per 1kb) with an average divergence to 90-125 of 7.63% (Supplementary file 3). These results indicate that *C. orthopsilosis* MCO456 is a hybrid between two parental lineages, one of which being very close to Type 2 strains such as 90-125. The other haplotype, which contains the ITS region and the MAT locus, would correspond to a parental that would have been classified as Type 1 subspecies (Supplementary figures S2 and S3). In fact the MTL locus of MCO456 has an α idiomorph, and is 100% identical to Cp289 Type 1 strain. In contrast, this locus has 95.34% divergence to the α idiomorph of Type 2 strains (represented by strain Cp185). 90-125 is a MTL α idiomorph. On the other hand, rDNA clusters of 90-125 and MCO456 are both homozygous and very similar similar in sequence, pointing to an origin of the rDNA in cluster in the hybrid from the Type 2 parental (Supplementary file 3). To estimate ploidy level in the putative hybrid, we investigated the distribution of read counts at biallelic SNPs for each mapped chromosomes. In a diploid genome, the mean of read counts at heterozygous positions should have a single mode around 0.5, while we would expect two modes, 0.33 and 0.67, for triploids, and three modes, 0.25, 0.5 and 0.75 for tetraploids (Yoshida et al. 2013). Our results revealed a single peak around 0.5, indicating MCO456 is a diploid and no sign for large-scale aneuploidy is present in any of the chromosomes (Supplementary figure S5).

Interestingly, mitochondrial genomes of both strains are homogeneous, with no sequence variation detected even at the high resolution employed ($> 5600\times$ sequence coverage of the

mitochondrial genome). In addition the mitochondrial sequences from both strains are very similar in sequence, with 70-77 SNPs in the entire mitochondrial genome, corresponding to 0.3% divergence. This indicates that the mitochondrion from MCO456 was entirely inherited from the Type 2 parental. This result is consistent with uniparental mitochondrion inheritance within *Candida* spp. (Ni et al. 2011), although previous observations of chimeric sequences in *C. orthopsilosis* mitochondrial genomes (Valach et al. 2012) suggest that recombination could also occur between the two parental mitochondrial genomes. Altogether our results point to a chimeric genome of MCO456 with two distinct haplotypes at ~5% divergence. One of these two haplotypes contains a MAT locus identical to that of Type I strains, whereas the rDNA locus and the mitochondrial genome are nearly identical to those in Type II strains.

Admittedly, the lack of a fully-sequenced, homozygous Type 1 genome prevent us from fully describing one of the parentals. However, alternative hypotheses for the formation of this architecture that do not involve the hybridization of two genomes differing by ~5%, seem less plausible and are not compatible with the data presented. For instance, a whole genome duplication followed by divergence is not consistent with the lack of large blocks of conserved synteny, as detected in *S. cerevisiae*, or with a finding of a higher similarity of one of the haplotypes and the mitochondrial genome with another strain. Similarly, one could think of 90-125 as a derivative, by massive loss of heterozygosity from a highly heterozygous strain, but this strain has a different MTL idiomorph. Furthermore the existence of loss of massive heterozygosity in one strain does not explain the origin of heterozygosity in the first place, and, considering the divergence detected, would invoke massive loss of heterozygosity in a very short

time span. Finally, we investigated the sporulation ability of the hybrid strain on various media, pH, temperature and incubation time (see Materials and Methods). Microscopic observation revealed no ascospore formation in the cultures, thus no sporulation could be induced in the hybrid strain under the conditions we tested. However, considering the difficulty of studying this process in *Candida* spp (Sai et al. 2011), these results should not be considered definitive.

In its present evolutionary state, 17% of the sequenced hybrid genome for which we can assign an haplotype has conserved heterozygous regions from its two parentals, whereas 32% and 41% of the genome was inherited from either the Type 1 or Type 2 parental, respectively (Figure 1B). Of note, this roughly balanced distribution of genomic regions inherited from both parentals contrasts with a previously reported inter-species hybrid within the “CTG” clade, that of *Pichia (Meyerozyma) sorbitophila*, where a high unbalance between both parentals (36% to 5%) was found (Louis et al. 2012). This difference may be explained by the lower genetic divergence between parentals in the *C. orthopsilosis* case (5%, as compared to 15% in *M. sorbitophila*), which will result in a lower risk of genetic incompatibility (Bateson-Dobzhansky-Muller effect) (Cutter 2012). In such a case, loss of heterozygosity towards any of the parental haplotypes would be expected to evolve nearly neutrally. Consistent with this idea, we did not find any functional enrichment among genes present in each of the three genotypic categories. Furthermore, considering that we did not find large deletions, the erosion of the differences between parental chromosomes seems mainly due to homologous recombination between the two haplotypes initially present in distinct homeologous chromosomes. Consistent with this we identified numerous genome regions where the existence of past recombination events is supported at the sequence-level (see Supplementary file 4). Repeated recombination between

homeologous chromosomes would result in the current observed pattern with extensive regions of loss of heterozygosity and different haplotypes present in the same chromosome. Recombination can occur in both meiotic (sexual recombination) and mitotic cells, but they leave different genomic signatures that can be recognized with re-sequencing data. Indeed, in the case of sexual recombination we expect chromosome size to have a negative correlation with the length of LOH tracks and a positive correlation with levels of heterozygosity, because recombination rate per basepair increases with chromosome size (Yin & Petes 2013). In contrast, mitotic recombination will leave the opposite trend. Our results (Supplementary figure S6) show a negative correlation of the length of LOH tracks with chromosome size (Spearman's $r=-0.76$, $p<0.05$), and a positive correlation of the fraction of heterozygous sites with chromosome size (Spearman's $r=0.71$, $p<0.05$). Thus our results suggest a significant role of meiotic recombination in shaping the current hybrid structure and provides evidence for the existence of sexual recombination in *C. orthopsilosis*.

Global spread and virulence of a type 1-2 hybrid lineage

We sought further evidence of hybrid strains in *C. orthopsilosis* by inspecting the available genomic sequence of AY2 strain, isolated from a persistent skin infection in Singapore (Chan, GF et al. 2011), Genbank AMDC00000000). Strikingly, this strain was found to represent a very similar hybrid to MCO456, with regions of homozygosity and heterozygosity showing a high level of overlap and limited divergence at the sequence level between AY2 and MCO456 (99.997% identity at the nucleotide level). This indicates that these geographically distant

clinical isolates are highly related and derive from the same ancestral hybridization event. It remains to be established whether such hybridization event may have facilitated the persistence and spread of this clade with demonstrated virulence. We reconstructed the phylogenetic relationships between all *C. orthopsilosis* haplotypes by using 1,432,069 sites in common heterozygous regions in MCO456 and AY2 (Figure 1C). With the current genomic sampling, we cannot determine the exact origin of the hybrid lineage which should have happened somewhere before the separation of MCO456/AY2 and after their divergence from the 90-125 lineage. Note that the level of sequence divergence between MCO456 and AY2 is too close to the error rate of current sequencing technologies to properly estimate their time of divergence. Moreover, we found that regions of heterozygosity were almost completely overlapping with minor differences possible due to assembly errors. It is remarkable that two independent isolates from the same hybrid lineages have been found in opposite sides of the globe and that they are both related to infection episodes. This indicates that the hybrid line is virulent and that it has spread.

Concluding remarks

We investigated the extent of genome-wide divergence among two recognized subspecies of *C. orthopsilosis*, by sequencing an isolate classified as Type 1 subspecies and comparing it to the Type 2 sequenced isolate. Unexpectedly we found that the selected isolate was a hybrid of the two subspecies under study. This conclusion is strongly supported by the presence of a highly heterozygous genome in which one of the haplotypes is largely similar to the Type 1 sequenced isolate, whereas the other haplotype, which contains the Type-1 defining MAT and ITS loci has an average divergence of 5%. In addition, the hybrid genome was found to be diploid, and showing patterns of heterozygosity compatible with the effect of meiotic recombination. This

discovery suggests the existence of mating between distinct *C. orthopsilosis* lineages, supporting previous indications (Tavanti et al. 2007), and arguing against recent speculations of a lack of recombination within *C. orthopsilosis* (Sai et al. 2011; Riccombeni et al. 2012). Furthermore the hybrid originates from two relatively distant lineages, which underscores the importance of hybridization as an evolutionary mechanism having a role in the *Candida* clade. Considering that cells from *Candida* species respond to mating pheromones of different species within the clade, our results anticipate the possibility of finding more hybrids within this pathogenic group of species. These mechanisms can have important implications in how relevant virulence phenotypes such as adhesion capabilities or drug resistance could evolve within pathogenic lineages. Hybridization has been recently recognized as an important and widespread process in fungi, but its relevance for pathogenesis remains largely unexplored (Morales & Dujon 2012; Xu et al. 2002; González et al. 2006). Finally, we show that two clinical strains isolated in very distant geographical locations (Texas and Singapore) are close representatives of the same hybrid lineage. This demonstrates that the hybrid lineage is pathogenic and distributed globally. The significance of this finding, -two of the three clinical independent (and distant) isolates are from the same hybrid lineage - raises the question of whether hybridization and virulence properties are related. It is tempting to speculate that hybridization may have conferred some sort of selective advantage in the environment that have facilitated its spread, while additionally conferring increased virulence properties. We indeed detected that the hybrid presents higher copy numbers in genes related to pathogenesis such as efflux pumps or secreted lipases. Conversely one may wonder whether the stressful conditions in the host may have facilitated the formation of hybrids. Hybridization can trigger the formation of new species that can display unique phenotypic features, and this mechanism has been proposed to play a role in the

emergence of globally-spread virulent lineages in other fungal pathogens (Stukenbrock et al. 2012). Certainly our current genomic sampling and limited availability of population and phenotypic data prevents us from providing definitive answers to many of these questions. Further research is thus needed to address these questions, including the direct comparison of virulence and anti-fungal resistance of the two sequenced strains.

Acknowledgements

The authors wish to thank Heinz Himmelbauer and the genomics facility at CRG for their technical assistance. We are thankful to Geraldine Butler for providing raw reads of the 90-125 strain. TG group research is funded in part by a grant from the Spanish ministry of Economy and Competitiveness (BIO2012-37161), a Grant from the Qatar National Research Fund grant (NPRP 5-298-3-086), and a grant from the European Research Council under the European Union's Seventh Framework Programme (FP/2007-2013) / ERC (Grant Agreement n. ERC-2012-StG-310325). LPP is funded through La Caixa-CRG International Fellowship Program. TN was supported by the TÁMOP 4.2.4. A/2-11-1-2012-001 “National Excellence Program”. AG was supported in part by OTKA NF 84006, NN00374 (ERA-Net PathoGenomics Program), EMBO Installation Grant and by the Janos Bolyai Fellowship of the Hungarian Academy of Sciences.

Figures and Table legends

Figure 1 *Candida orthopsilosis* MCO456 is a hybrid of two subspecies

Distribution of number of SNPs between 1kb homozygous regions of MCO456 and 90-125 is bimodal, with peaks around 0.3% and above 3% inter-strain divergence (A). The genome of MCO456 can be assigned into four categories: haplotype A (close in sequence to 90-125, therefore Type 2), haplotype B (Type 1), heterozygous, and unknown (B). The distance between the two haplotypes in heterozygous regions of MCO456 and AY2 is larger than distances between strains, but smaller than distance to the closest species, therefore we hypothesize MCO456 is hybrid of two *C. orthopsilosis* subspecies (C).

Figure 2 Copy number differences between *C. orthopsilosis* strains

Two duplications, DUP28 (A) and DUP4 (B), were analysed in detail (marked with red rectangles). For each duplication ten panels are given in this order, from top to down: genomic coordinates; genomic coverage, genomic reads alignments and split-read mapping for 90-125; genomic coverage, genomic reads alignments and split-read mapping for MCO456; transcriptomic coverage and transcriptomic reads alignments from MCO456; and predicted loci. Both regions, DUP28 and DUP4, are fully homozygous and present in twelve copies in the genome as compared to two in *C. orthopsilosis* 90-125 reference genome. All copies of DUP4 are most likely in tandem, while copies of DUP28 are spread through at least five chromosomes. A genes encoded within DUP28 (CORT_0H02780, which encodes a putative outer-membrane Na/K efflux pump) and DUP4 (CORT_0A11440, which encodes a vacuolar transporter), are expressed at higher levels, as compared to their neighboring genes.

Table 1 Genome sequencing stats

Basic strain and assembly statistics for the genome obtained within this work, the reference strain and an assembly available in GenBank (AMDC00000000). For each strain the table provides, in this order: strain name; geographical origin; number of reads obtained, average coverage (x fold); number of scaffolds; total assembly size; GC content; number of bases in gaps; number of predicted genes; number of homozygous and heterozygous sites. Note that the highly fragmented nature of the AY2 assembly is likely due to the fact that high heterozygosity was not specifically taken care of as we do here.

sample	origin	# reads [million s]	depth of coverag e	scaff olds	assemb ly size [kb]	GC [%]	Ns	gene s	hom o SNPs	hetero SNPs
90-125	USA, San Francisc o	35.32	235	8	12,659	37.4 6	177,2 68	5,70 0	872	1,184
MCO45 6	USA, San Antonio	90.22	544	116	13,272	34.4 2	1,453	5,75 6	92,49 7	197,53 1
AY2	Singapor e	-	-	4,152	14,511	37.3 1	0	-	-	-

List of supplementary files

Supplementary file 1: Supplementary figures

Supplementary file 2: Supplementary tables

Supplementary Table S1: List of gene number differences among the 2 strains

The table lists groups of orthologous genes that differ in copy number between two *C. orthopsilosis* strains and *C. parapsilosis*. For each orthologous group, unique identifier, size of orthologous group, number of members and their names from *C. orthopsilosis* 90-125 (CANOR), *C. parapsilosis* CDC317 (CANPA) and *C. orthopsilosis* MCO456 (MCO456), functions associated with members of each orthologous group and difference in group size between MCO456 and 90-125 are given. Orthologs of *C. albicans* genes implicated in cellular response to drug (GO:0035690) are annotated with `drug response`. Orthologous clusters important to virulence are marked with colors.

Supplementary Table S2: structural variations: duplications

For each duplication, the duplication size (~ marks estimated size, otherwise the precise size is given), affected strain (duplications in both, 90-125 and MCO456 were detected), observed ploidy (2x denotes wild-type, as *C. orthopsilosis* is diploid), affected genes and their functions are given. In addition, we commented on some interesting features and provided independent InterPro annotation. Common or strain-specific duplications are marked in different colors.

Supplementary Table S3: structural variations: deletions

For each deletion in *C. orthopsilosis* MCO456, the deletion size (~ marks estimated size, otherwise precise size is given), affected genes, the size of repeat (if observed deletion was caused by DBS followed by single strand annealing repair), information about ploidy (null or heterozygous deletion), observed gene fusions (also including promoter regions) and putative functions of lost genes are given. In the last column, we commented on the position of the deletion in coding region and possible effect if the deletion did not affect entire gene. Deletions are color-coded based on their effect.

Supplementary Table S4: Genes affected by the largest duplications (DUP2)

Table lists 74 genes duplicated due to the largest duplication (DUP2) and their functions.

Supplementary file 3

Candida orthopsilosis chromosomes graphs.

Supplementary file 4.

Regions with homologous recombination.

Literature cited

Angiuoli SV, Salzberg SL. 2011. Mugsy: fast multiple alignment of closely related whole genomes. *Bioinforma. Oxf. Engl.* 27:334–342. doi: 10.1093/bioinformatics/btq665.

Van Asbeck EC, Clemons KV, Stevens DA. 2009. *Candida parapsilosis*: a review of its epidemiology, pathogenesis, clinical aspects, typing and antimicrobial susceptibility. *Crit. Rev. Microbiol.* 35:283–309. doi: 10.3109/10408410903213393.

- Bertini A et al. 2013. Comparison of *Candida parapsilosis*, *Candida orthopsilosis*, and *Candida metapsilosis* adhesive properties and pathogenicity. *Int. J. Med. Microbiol. IJMM*. 303:98–103. doi: 10.1016/j.ijmm.2012.12.006.
- Binkley J et al. 2014. The *Candida* Genome Database: the new homology information page highlights protein similarity and phylogeny. *Nucleic Acids Res.* 42:D711–716. doi: 10.1093/nar/gkt1046.
- Boetzer M, Henkel CV, Jansen HJ, Butler D, Pirovano W. 2011. Scaffolding pre-assembled contigs using SSPACE. *Bioinforma. Oxf. Engl.* 27:578–579. doi: 10.1093/bioinformatics/btq683.
- Bonfietti LX et al. 2012. Prevalence, distribution and antifungal susceptibility profiles of *Candida parapsilosis*, *Candida orthopsilosis* and *Candida metapsilosis* bloodstream isolates. *J. Med. Microbiol.* 61:1003–1008. doi: 10.1099/jmm.0.037812-0.
- Butler G et al. 2009. Evolution of pathogenicity and sexual reproduction in eight *Candida* genomes. *Nature*. 459:657–662. doi: 10.1038/nature08064.
- Chan, GF, Gan, HM, Puad, MSA, Rashid, NAA. 2011. *Candida orthopsilosis* and *Aureobasidium pullulans*: Rare Fungal Pathogens Causing Persistent Skin Infection. *Insight Infect. Dis.* 1:1–4.
- Cutter AD. 2012. The polymorphic prelude to Bateson-Dobzhansky-Muller incompatibilities. *Trends Ecol. Evol.* 27:209–218. doi: 10.1016/j.tree.2011.11.004.
- Gácsér A, Stehr F, et al. 2007. Lipase 8 affects the pathogenesis of *Candida albicans*. *Infect. Immun.* 75:4710–4718. doi: 10.1128/IAI.00372-07.
- Gácsér A, Schäfer W, Nosanchuk JS, Salomon S, Nosanchuk JD. 2007. Virulence of *Candida parapsilosis*, *Candida orthopsilosis*, and *Candida metapsilosis* in reconstituted human tissue models. *Fungal Genet. Biol. FG B.* 44:1336–1341. doi: 10.1016/j.fgb.2007.02.002.
- Gácsér A, Trofa D, Schäfer W, Nosanchuk JD. 2007. Targeted gene deletion in *Candida parapsilosis* demonstrates the role of secreted lipase in virulence. *J. Clin. Invest.* 117:3049–3058. doi: 10.1172/JCI32294.
- Ge YP et al. 2012. Characterization of the *Candida parapsilosis* complex in East China: species distribution differs among cities. *Med. Mycol.* 50:56–66. doi: 10.3109/13693786.2011.591440.
- Ghannoum MA et al. 2010. Characterization of the oral fungal microbiome (mycobiome) in healthy individuals. *PLoS Pathog.* 6:e1000713. doi: 10.1371/journal.ppat.1000713.
- González SS, Barrio E, Gafner J, Querol A. 2006. Natural hybrids from *Saccharomyces cerevisiae*, *Saccharomyces bayanus* and *Saccharomyces kudriavzevii* in wine fermentations. *FEMS Yeast Res.* 6:1221–1234. doi: 10.1111/j.1567-1364.2006.00126.x.
- Horváth P, Nosanchuk JD, Hamari Z, Vágvölgyi C, Gácsér A. 2012. The identification of gene duplication and the role of secreted aspartyl proteinase 1 in *Candida parapsilosis* virulence. *J. Infect. Dis.* 205:923–933. doi: 10.1093/infdis/jir873.
- Huang S et al. 2012. HaploMerger: reconstructing allelic relationships for polymorphic diploid genome assemblies. *Genome Res.* 22:1581–1588. doi: 10.1101/gr.133652.111.

- Ivanov EL, Sugawara N, Fishman-Lobell J, Haber JE. 1996. Genetic requirements for the single-strand annealing pathway of double-strand break repair in *Saccharomyces cerevisiae*. *Genetics*. 142:693–704.
- Langmead B, Salzberg SL. 2012. Fast gapped-read alignment with Bowtie 2. *Nat. Methods*. 9:357–359. doi: 10.1038/nmeth.1923.
- Li H, Durbin R. 2010. Fast and accurate long-read alignment with Burrows-Wheeler transform. *Bioinforma. Oxf. Engl.* 26:589–595. doi: 10.1093/bioinformatics/btp698.
- Lockhart SR, Messer SA, Pfaller MA, Diekema DJ. 2008. Geographic distribution and antifungal susceptibility of the newly described species *Candida orthopsilosis* and *Candida metapsilosis* in comparison to the closely related species *Candida parapsilosis*. *J. Clin. Microbiol.* 46:2659–2664. doi: 10.1128/JCM.00803-08.
- Louis VL et al. 2012. *Pichia sorbitophila*, an Interspecies Yeast Hybrid, Reveals Early Steps of Genome Resolution After Polyploidization. *G3 Bethesda Md.* 2:299–311. doi: 10.1534/g3.111.000745.
- Luo R et al. 2012. SOAPdenovo2: an empirically improved memory-efficient short-read de novo assembler. *GigaScience*. 1:18. doi: 10.1186/2047-217X-1-18.
- Martel CM et al. 2010. Identification and Characterization of Four Azole-Resistant *erg3* Mutants of *Candida albicans*. *Antimicrob. Agents Chemother.* 54:4527–4533. doi: 10.1128/AAC.00348-10.
- McKenna A et al. 2010. The Genome Analysis Toolkit: a MapReduce framework for analyzing next-generation DNA sequencing data. *Genome Res.* 20:1297–1303. doi: 10.1101/gr.107524.110.
- Monod M, Borg-von ZM. 2002. Secreted aspartic proteases as virulence factors of *Candida* species. *Biol. Chem.* 383:1087–1093. doi: 10.1515/BC.2002.117.
- Morales L, Dujon B. 2012. Evolutionary role of interspecies hybridization and genetic exchanges in yeasts. *Microbiol. Mol. Biol. Rev. MMBR.* 76:721–739. doi: 10.1128/MMBR.00022-12.
- Naglik JR, Challacombe SJ, Hube B. 2003. *Candida albicans* secreted aspartyl proteinases in virulence and pathogenesis. *Microbiol. Mol. Biol. Rev. MMBR.* 67:400–428, table of contents.
- Németh T et al. 2013. Characterization of virulence properties in the *C. parapsilosis sensu lato* species. *PloS One*. 8:e68704. doi: 10.1371/journal.pone.0068704.
- Ni M, Feretzaki M, Sun S, Wang X, Heitman J. 2011. Sex in fungi. *Annu. Rev. Genet.* 45:405–430. doi: 10.1146/annurev-genet-110410-132536.
- Orsi CF, Colombari B, Blasi E. 2010. *Candida metapsilosis* as the least virulent member of the ‘*C. parapsilosis*’ complex. *Med. Mycol. Off. Publ. Int. Soc. Hum. Anim. Mycol.* 48:1024–1033. doi: 10.3109/13693786.2010.489233.
- Pryszcz LP, Huerta-Cepas J, Gabaldón T. 2011. MetaPhOrs: orthology and paralogy predictions from multiple phylogenetic evidence using a consistency-based confidence score. *Nucleic Acids Res.* 39:e32. doi: 10.1093/nar/gkq953.

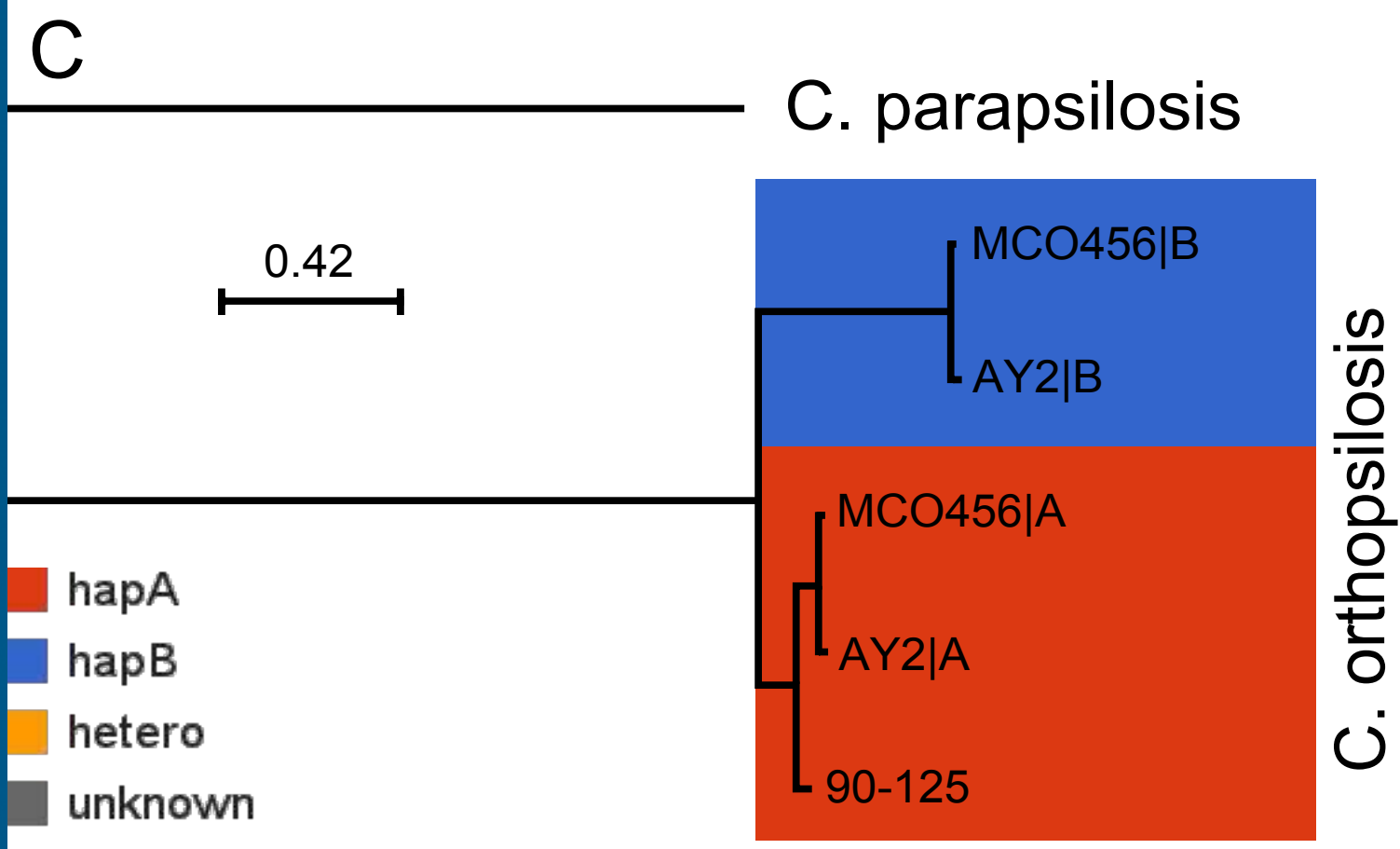
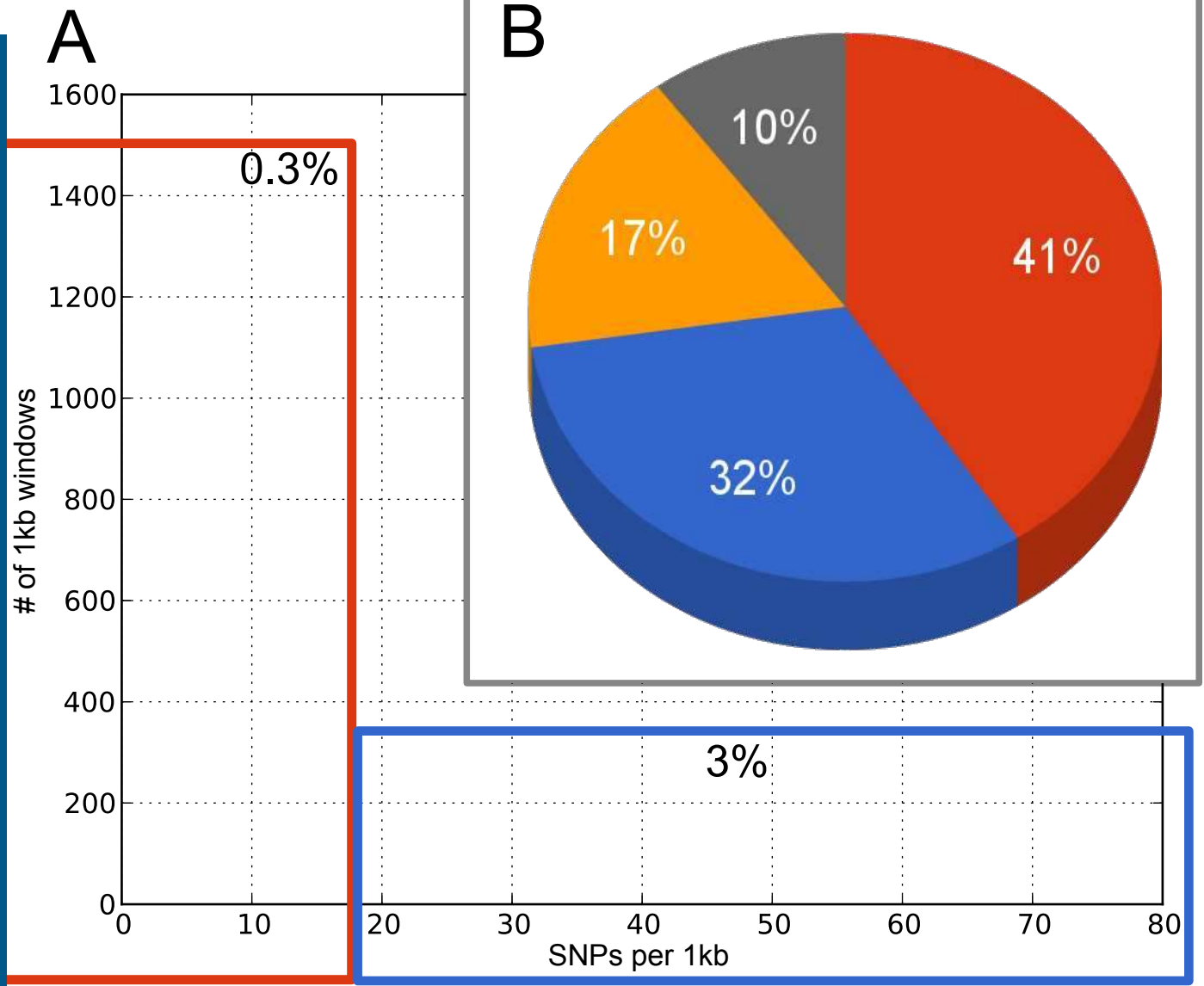
- Pryszcz LP, Németh T, Gácsér A, Gabaldón T. 2013. Unexpected genomic variability in clinical and environmental strains of the pathogenic yeast *Candida parapsilosis*. *Genome Biol. Evol.* doi: 10.1093/gbe/evt185.
- Quevillon E et al. 2005. InterProScan: protein domains identifier. *Nucleic Acids Res.* 33:W116–120. doi: 10.1093/nar/gki442.
- Rausch T et al. 2012. DELLY: structural variant discovery by integrated paired-end and split-read analysis. *Bioinforma. Oxf. Engl.* 28:i333–i339. doi: 10.1093/bioinformatics/bts378.
- Riccombeni A, Vidanes G, Proux-Wéra E, Wolfe KH, Butler G. 2012. Sequence and analysis of the genome of the pathogenic yeast *Candida orthopsilosis*. *PloS One.* 7:e35750. doi: 10.1371/journal.pone.0035750.
- Richter DC, Schuster SC, Huson DH. 2007. OSLay: optimal syntenic layout of unfinished assemblies. *Bioinforma. Oxf. Engl.* 23:1573–1579. doi: 10.1093/bioinformatics/btm153.
- Sai S, Holland LM, McGee CF, Lynch DB, Butler G. 2011. Evolution of mating within the *Candida parapsilosis* species group. *Eukaryot. Cell.* 10:578–587. doi: 10.1128/EC.00276-10.
- Stamatakis A, Ludwig T, Meier H. 2005. RAxML-III: a fast program for maximum likelihood-based inference of large phylogenetic trees. *Bioinforma. Oxf. Engl.* 21:456–463. doi: 10.1093/bioinformatics/bti191.
- Stanke M et al. 2006. AUGUSTUS: ab initio prediction of alternative transcripts. *Nucleic Acids Res.* 34:W435–439. doi: 10.1093/nar/gkl200.
- Stukenbrock EH, Christiansen FB, Hansen TT, Dutheil JY, Schierup MH. 2012. Fusion of two divergent fungal individuals led to the recent emergence of a unique widespread pathogen species. *Proc. Natl. Acad. Sci. U. S. A.* 109:10954–10959. doi: 10.1073/pnas.1201403109.
- Szenzenstein J et al. 2013. Differential sensitivity of the species of *Candida parapsilosis sensu lato* complex against statins. *Mycopathologia.* 176:211–217. doi: 10.1007/s11046-013-9689-1.
- Taj-Aldeen SJ et al. 2013. Epidemiology of candidemia in Qatar, the Middle East: performance of MALDI-TOF MS for the identification of *Candida* species, species distribution, outcome, and susceptibility pattern. *Infection.* doi: 10.1007/s15010-013-0570-4.
- Tavanti A, Davidson AD, Gow NAR, Maiden MCJ, Odds FC. 2005. *Candida orthopsilosis* and *Candida metapsilosis* spp. nov. To Replace *Candida parapsilosis* Groups II and III. *J. Clin. Microbiol.* 43:284–292. doi: 10.1128/JCM.43.1.284-292.2005.
- Tavanti A, Hensgens LAM, Ghelardi E, Campa M, Senesi S. 2007. Genotyping of *Candida orthopsilosis* Clinical Isolates by Amplification Fragment Length Polymorphism Reveals Genetic Diversity among Independent Isolates and Strain Maintenance within Patients. *J. Clin. Microbiol.* 45:1455–1462. doi: 10.1128/JCM.00243-07.
- Valach M et al. 2012. Mitochondrial genome variability within the *Candida parapsilosis* species complex. *Mitochondrion.* 12:514–519. doi: 10.1016/j.mito.2012.07.109.

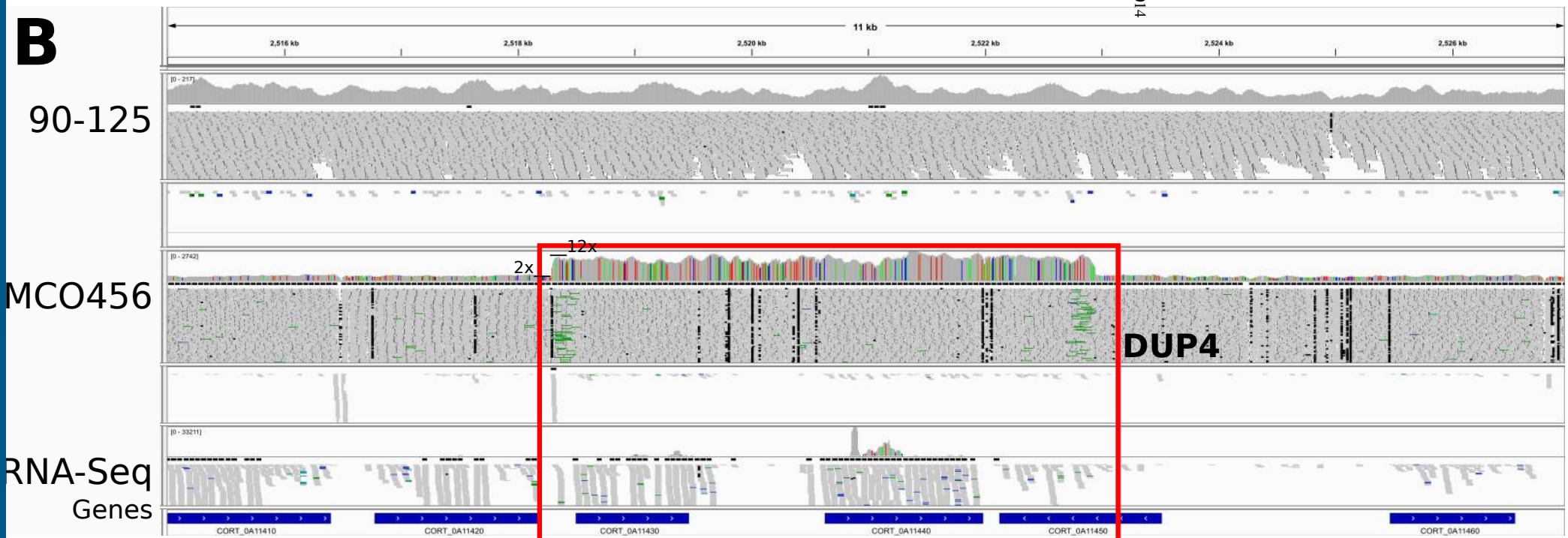
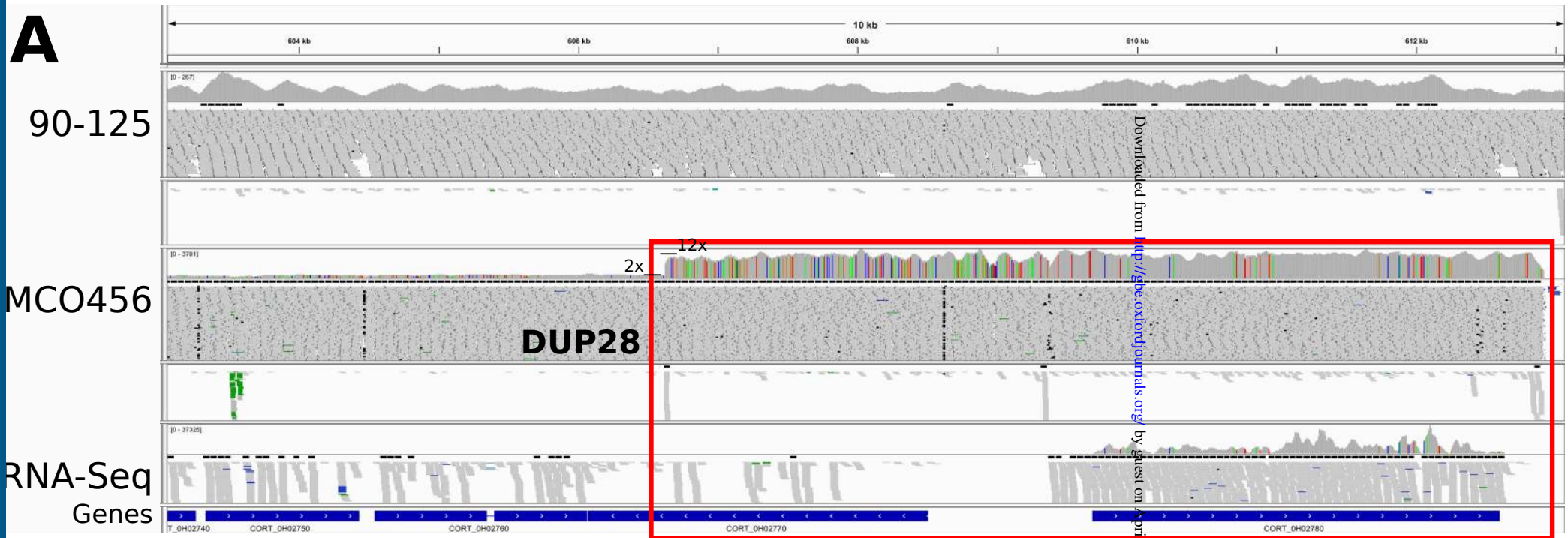
Xu D et al. 2007. Genome-wide fitness test and mechanism-of-action studies of inhibitory compounds in *Candida albicans*. *PLoS Pathog.* 3:e92. doi: 10.1371/journal.ppat.0030092.

Xu J, Luo G, Vilgalys RJ, Brandt ME, Mitchell TG. 2002. Multiple origins of hybrid strains of *Cryptococcus neoformans* with serotype AD. *Microbiol. Read. Engl.* 148:203–212.

Yin Y, Petes TD. 2013. Genome-Wide High-Resolution Mapping of UV-Induced Mitotic Recombination Events in *Saccharomyces cerevisiae*. *PLoS Genet.* 9. doi: 10.1371/journal.pgen.1003894.

Yoshida K et al. 2013. The rise and fall of the *Phytophthora infestans* lineage that triggered the Irish potato famine. *eLife.* 2. doi: 10.7554/eLife.00731.





Downloaded from <http://gbe.oxfordjournals.org/> by guest on April 24, 2014